Progress In Electromagnetics Research, PIER 90, 205–217, 2009

PILOT AND DATA SYMBOL-AIDED FREQUENCY ESTIMATION FOR UWB-OFDM

Y.-H. You

uT Communication Research Center
Sejong University
98 Kunja-Dong, Kwangjin-Ku, Seoul 143-747, Korea

J. B. Kim

Nortel Networks, 2201 Lakeside Blvd.
Richardson, TX' 75082, USA

Abstract—In this paper, an improved residual carrier frequency offset estimation scheme is proposed for ultra-wideband multiband orthogonal frequency division multiplexing (UWB-OFDM) systems. The basic idea of our approach is based on the fact that two adjacent OFDM symbols convey identical information in an UWB-OFDM system. The mean square error of the synchronization scheme is derived, and its simple expression is also calculated. Finally, simulation results are demonstrated to verify the theoretical analysis in this paper.

1. INTRODUCTION

Ultra wideband (UWB) radio signals employ the transmission of very short impulses of radio energy whose characteristic spectrum signature extends across a wide range of radio frequencies [1–3]. A traditional UWB technology is based on single-band systems employing carrier-free communications [4–6]. Recently, multi-band orthogonal frequency division multiplexing (MB-OFDM) systems have attracted much research attention and have been adopted as standards for the high-rate UWB physical layer [4].

In UWB-OFDM, frequency hopping is combined with OFDM for high data-rate transmission over wireless channels. Although this technique is very promising, the disadvantages of OFDM are also

Corresponding author: Y.-H. You (yhyou@sejong.ac.kr).

inherent in UWB-OFDM [8, 9]. One of those limitations of MB-OFDM is its sensitivity to frequency synchronization errors [5, 6]. Both residual carrier frequency offset (CFO) and sampling frequency offset (SFO) arise from by small differences in oscillator frequencies between the transmitter and receiver, which causes time and subcarrier variant phase rotations and fast Fourier transform (FFT) window shift. A number of algorithms to combat the frequency error, which use pilot subcarriers, are presented in [7, 8]. In the UWB-OFDM system [4], only a few pilots are embedded for frequency tracking. Therefore, increasing the accuracy of carrier-frequency estimation with the limited number of pilots is one of the major concerns for the UWB-OFDM systems.

This paper proposes a CFO estimation algorithm by exploiting the inherent repetition information of UWB-OFDM signals, thereby both pilot and data symbols are used to estimate the frequency offset. Analytical derivation and simulation for mean square error (MSE) are provided. Based on the analysis and simulation, it is shown that the proposed CFO estimator achieves better MSE performance at the expense of the reduced estimation range, compared to a pilot-assisted conventional estimator [7].

This paper is organized as follows: Section 2 describes the signal model for the UWB-OFDM system. In Section 3, an improved CFO estimation scheme is suggested for UWB-OFDM and its performance is derived in terms of MSE. In Section 4, we then present simulation results to verify the performance of the frequency estimator, and we conclude this paper with Section 5.

2. SYSTEM MODEL

In the UWB-OFDM system, N complex symbols are modulated onto N sub-carriers by using the inverse FFT at the transmitter and N_g samples are zero-padded to form a guard interval. In the UWB-OFDM system, both frequency domain spreading (FDS) and time domain spreading (TDS) techniques can be used when the data is encoded at the rate of 53.3 or 80 Mb/s. When the data is encoded at the rate of 106.7, 160 or 200 Mb/s, only TDS technique is adopted. In all transmission modes, a pair of two consecutive OFDM symbols denoted by $\{X_{2l}(k), X_{2l+1}(k)\}$ conveys the same information.

After compensating the carrier frequency offset with initial packet/frame synchronization sequence [5, 6], residual CFO and SFO may not be completely removed. Thus, after FFT demodulation, small

SFO Δ_s and residual CFO Δ_r are presented in the received signal [9, 10]

$$R_{2l+n}(k) \approx SC_{b(2l+n)}(k)X_{2l+n}(k)e^{j2\pi(K_{b(2l+n)}\Delta_r+M(k)\Delta_s)(2l+n)N_e/N} + W_{2l+n}(k),\ 0 \le k \le N_d + N_p - 1,\ n = 0,\ 1 \quad (1)$$

where the symbol index l ranges from $-\infty$ to ∞, S is the log-normal shadowing term, $X_{2l+n}(k)$ is the OFDM symbol transmitted on the k-th subcarrier at the $(2l+n)$-th symbol period, $b(2l+n) \in \{1, 2, 3\}$ is the identification of the frequency band occupied by the $(2l+n)$-th symbol, $C_{b(2l+n)}(k)$ is the channel frequency response incorporating the time-invariant phase with zero mean and variance σ_C^2 at the frequency band $b(2l+n)$, $N_e = N + N_g$, and $W_{2l+n}(k)$ is a zero-mean complex Gaussian noise term with variance σ_W^2.

In (1), N_p is the number of pilot subcarriers, N_d is the number of data samples in one OFDM symbol excluding the guard subcarriers, $M(k)$ is a mapping function from indice $[0, N_d + N_p - 1]$ to the logical frequency subcarriers $[-(N_d + N_p)/2,\ (N_d + N_p)/2]$ excluding zero as specified in [4], and $K_{b(2l+n)}$ is a real constant depending on implementations of carrier frequencies generation. In this paper, assuming the carrier frequency synthesizer for mode 1 of the UWB-OFDM system, $[K_1, K_2, K_3] = [13/16, 15/16, 17/16]$ is considered [6].

3. CFO ESTIMATION SCHEME FOR UWB-OFDM

In order to estimate the frequency error with the help of data symbols, a simple way of implementing a fine frequency estimator is suggested in this section and its estimation performance is analytically derived.

3.1. Estimation Algorithm

The UWB-OFDM specification in [4] provides 10 different time-frequency codes (TFC's) from TFC1 to TFC10 and these codes provide frequency hopping from a sub-band to another at the end of each OFDM symbol. Figure 1 shows the transmitted signal when the UWB-OFDM system uses TFC1 or TFC8. As shown in Figure 1, there is the periodicity D_1 (measured in OFDM symbols) of the sequence of the band-id pairs $[b(2l), b(2l+1)]$ occupied by two consecutive OFDM symbols for a given band-hopping pattern or TFC. Therefore, we can observe

$$[b(2l+m_1D_1), b(2l+m_1D_1+1)] = [b(2l+m_2D_1), b(2l+m_2D_1+1)] \quad (2)$$

where m_1 and m_2 are integer-valued that meet $m_2 > m_1$. Note that the parameter D_1 depends on the TFCs, i.e., $D_1 = 6$ for TFCs 1$\sim$4

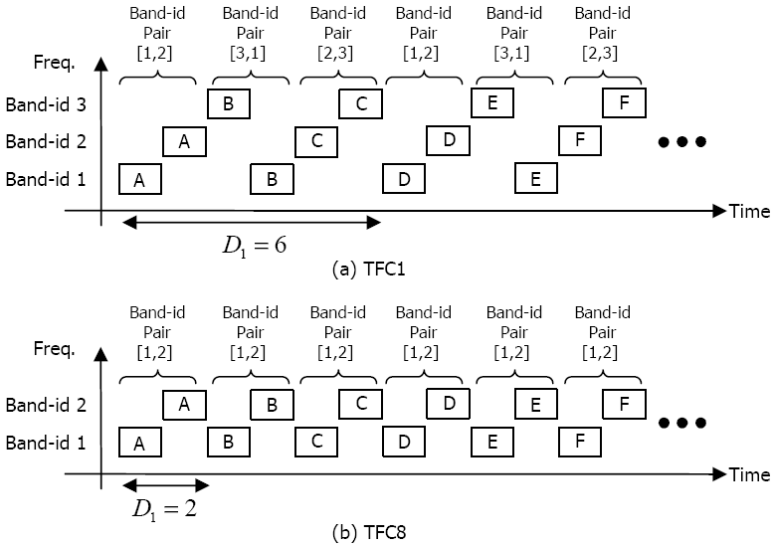

Figure 1. Transmitted signals for TFC1 and TFC8.

and $D_1 = 2$ for TFCs 5∼10 [4]. In order to estimate band-dependent CFO as in (1), the proposed scheme exploits the periodic nature of the band-id pairs.

For the transmission mode of UWB-OFDM that employs only TDS, two consecutive OFDM symbols are symmetrically related to each other by [4]

$$X_{2l+mD_1+1}(k) = X^{Q}_{2l+mD_1}(N_u - k - 1) + jX^{I}_{2l+mD_1}(N_u - k - 1) \quad (3)$$

where the subcarrier index ranges $0 \leq k \leq N_d + N_p - 1$, m is integer-valued, and $X^{I/Q}_{2l+mD_1}(k)$ are the real and imaginary parts of $X_{2l+mD_1}(k)$, respectively. Note that the relation (3) is valid for both pilot and data symbols. The subcarrier index $0 \leq k \leq N_d + N_p - 1$ and definition of m or m_i $(i = 1, 2)$ will be used in the reminder of this paper if not specified.

By using the relation between two consecutive symbols $X_{2l+mD_1}(k)$ and $X_{2l+mD_1+1}(k)$, it is clear that

$$X_{2l+mD_1}(N_u - k - 1)X_{2l+mD_1+1}(k) = j|X_{2l+mD_1}(N_u - k - 1)|^2 \quad (4)$$

where $N_u = N_d + N_p$. Denoting $\vartheta_{b(l)}(k) = (K_{b(l)}\Delta_r + M(k)\Delta_s)l$, we

obtain

$$\begin{aligned} T_{2l+mD_1}(k) &= (-j)Y_{2l+mD_1}(N_u-k-1)Y_{2l+mD_1+1}(k) \\ &= E_s e^{j2\pi[\vartheta_{b(2l+mD_1)}(N_u-k-1)+\vartheta_{b(2l+mD_1+1)}(k)]\rho} + \hat{W}_{2l+mD_1}(k) \end{aligned} \quad (5)$$

where

$$Y_{2l+mD_1+n}(k) = R_{2l+mD_1+n}(k)/\hat{H}_{b(2l+mD_1+n)}(k),\ n=0,\ 1 \quad (6)$$

is the compensated signal by the estimated channel, $E_s = |X_{2l+mD_1}(N_u-k-1)|^2$, $\rho = N_e/N$, $\hat{H}_{b(2l+mD_1)}(k)$ is the estimate of $H_{b(2l+mD_1)}(k) = SC_{b(2l+mD_1)}(k)$, and $\hat{W}_{2l+mD_1}(k)$ is the noise contribution caused by the additive noise and channel estimation (CE) error. The operation in (6) is well known as one-tap frequency-domain equalization [16]. Recalling from the definition of the mapping function $M(k)$ that $M(k)+M(N_u-k-1)=0$ [4], one can see in (5) that

$$\begin{aligned} &\vartheta_{b(2l+mD_1)}(N_u-k-1)+\vartheta_{b(2l+mD_1+1)}(k) \\ &= K_{b(2l+mD_1)}\Delta_r(2l+mD_1)+K_{b(2l+mD_1+1)}\Delta_r(2l+mD_1+1)+M(k)\Delta_s \end{aligned} \quad (7)$$

which yields

$$T_{2l+mD_1}(k) = E_s e^{j2\pi[\phi_{2l+mD_1}+M(k)\Delta_s]\rho} + \hat{W}_{2l+mD_1}(k) \quad (8)$$

where $\phi_{2l+mD_1} = K_{b(2l+mD_1)}\Delta_r(2l+mD_1) + K_{b(2l+mD_1+1)}\Delta_r(2l+mD_1+1)$.

We define a temporal correlation to derive the data-aided CFO estimator for UWB-OFDM

$$T^*_{2l+m_1D_1}(k)T_{2l+m_2D_1}(k) = E_s^2 e^{j2\pi[\phi_{2l+m_2D_1}-\phi_{2l+m_1D_1}]\rho} + \tilde{W}_{2l}(k) \quad (9)$$

where the noise contribution $\tilde{W}_{2l}(k)$ is given by

$$\begin{aligned} \tilde{W}_{2l}(k) \;=\; & E_s e^{-j2\pi(\phi_{2l+m_1D_1}+M(k)\Delta_s)\rho}\hat{W}_{2l+m_2D_1}(k) \\ & + E_s e^{j2\pi(\phi_{2l+m_2D_1}+M(k)\Delta_s)\rho}\hat{W}^*_{2l}(k) \\ & + \hat{W}^*_{2l+m_1D_1}(k)\hat{W}_{2l+m_2D_1}(k). \end{aligned} \quad (10)$$

Based on (2), $K_{b(2l+m_1D_1)} = K_{b(2l+m_2D_1)}$ and $K_{b(2l+m_1D_1+1)} = K_{b(2l+m_2D_1+1)}$, and it follows that

$$\phi_{2l+m_2D_1}-\phi_{2l+m_1D_1} = \Delta_r[K_{b(2l+m_1D_1)}+K_{b(2l+m_2D_1)}](m_2-m_1)D_1 \quad (11)$$

which yields

$$\begin{aligned} & T^*_{2l+m_1D_1}(k)T_{2l+m_2D_1}(k) \\ = \; & E_s^2 e^{j2\pi\Delta_r[K_{b(2l+m_1D_1)}+K_{b(2l+m_2D_1)}](m_2-m_1)D_1\rho} + \tilde{W}_{2l}(k). \end{aligned} \quad (12)$$

In an analogy to [7], an estimation of Δ_r is now obtained by

$$\hat{\Delta}_r = \frac{\sum_{k=0}^{N_u-1} \measuredangle \left\{T^*_{2l+m_1D_1}(k)T_{2l+m_2D_1}(k)\right\}}{2\pi N_u[K_{b(2l+m_1D_1)} + K_{b(2l+m_2D_1)}](m_2-m_1)D_1\rho} \quad (13)$$

with $\measuredangle$ denoting the angle of the complex number. Finally, our estimation of the residual CFO is obtained by averaging $\hat{\Delta}_r$ over all possible pairs of band-id's for a given TFC. As shown in Figure 1, there are three different band-id pairs for TFC1∼TFC4, while only one band-id pair exists in TFC5∼TFC10.

3.2. Performance Analysis

To derive the MSE of the proposed CFO estimator, we assume a perfect channel knowledge at the receiver. Then, $T_{2l+m_iD_1}(k)$ in (8) can be simply written by

$$T_{2l+m_iD_1}(k) = E_s e^{j2\pi(\phi_{2l+m_iD_1}+M(k)\Delta_s)\rho}\left[1+\mathcal{W}_{2l+m_iD_1}(k)\right], \; i=1,\,2 \quad (14)$$

where

$$\begin{aligned} & \mathcal{W}_{2l+m_iD_1}(k) \\ = \; & (-j)\frac{X_{2l+m_iD_1}(N_u-k-1)W_{2l+m_iD_1+1}(k)}{E_sH_{b(2l+m_iD_1+1)}(k)}e^{-j2\pi\vartheta_{b(2l+m_iD_1)}(N_u-k-1)\rho} \\ & +(-j)\frac{X_{2l+m_iD_1+1}(k)W_{2l+m_iD_1}(N_u-k-1)}{E_sH_{b(2l+m_iD_1)}(N_u-k-1)}e^{-j2\pi\vartheta_{b(2l+m_iD_1+1)}(k)\rho} \\ & +(-j)\frac{W_{2l+m_iD_1}(N_u-k-1)W_{2l+m_iD_1+1}(k)}{E_sH_{b(2l+m_iD_1)}(N_u-k-1)H_{b(2l+m_iD_1+1)}(k)}. \end{aligned} \quad (15)$$

Note that $\measuredangle\left\{T^*_{2l+m_1D_1}(k)T_{2l+m_2D_1}(k)\right\} = \measuredangle\{T_{2l+m_2D_1}(k)\} - \measuredangle\{T_{2l+m_1D_1}(k)\}$ and $\phi_{2l+m_2D_1} - \phi_{2l+m_1D_1} = \Delta_r[K_{b(2l+m_1D_1)} + K_{b(2l+m_2D_1)}](m_2-m_1)D_1$. By employing the approximation at high

SNR [11], the error of the estimate can be simplified as

$$\begin{aligned}\epsilon_\Delta &= \hat{\Delta}_r - \Delta_r \\ &\approx \frac{1}{2\pi N_u[K_{b(2l+m_1D_1)} + K_{b(2l+m_2D_1)}](m_2-m_1)D_1\rho} \\ &\cdot \left[\sum_{k=0}^{N_u-1} \mathcal{W}^Q_{2l+m_2D_1}(k) - \sum_{k=0}^{N_u-1} \mathcal{W}^Q_{2l+m_1D_1}(k)\right]. \end{aligned} \tag{16}$$

Based on $E\{\mathcal{W}^Q_{2l+m_1D_1}(k)\} = E\{\mathcal{W}^Q_{2l+m_2D_1}(k)\} = 0$, then, the MSE of CFO estimator can be expressed as

$$\begin{aligned}E\left\{|\epsilon_\Delta|^2\right\} \approx &\left(\frac{1}{2\pi N_u[K_{b(2l+m_1D_1)} + K_{b(2l+m_2D_1)}](m_2-m_1)D_1\rho}\right)^2 \\ &\cdot \sum_{k=0}^{N_u-1}\left[E\left\{\left|\mathcal{W}^Q_{2l+m_2D_1}(k)\right|^2\right\} + E\left\{\left|\mathcal{W}^Q_{2l+m_1D_1}(k)\right|^2\right\}\right]. \end{aligned} \tag{17}$$

Since we assume that $H_{b(2l+m_1D_1)}(N_u-k-1)$ and $H_{b(2l+m_2D_1)}(k)$ are highly uncorrelated in frequency in (15) even when TFCs 3∼7 are used [10], after simple manipulation, the variance of the noise in (15) is given by

$$\begin{aligned}&E\left\{\left|\mathcal{W}^Q_{2l+m_iD_1}(k)\right|^2\right\} = \frac{\sigma_W^2}{E_s} E\left\{\frac{1}{|H_{b(2l+m_iD_1)}(N_u-k-1)|^2}\right\} \\ &+\frac{\sigma_W^4}{4E_s^2} E\left\{\frac{1}{|H_{b(2l+m_iD_1)}(N_u-k-1)|^2}\right\} E\left\{\frac{1}{|H_{b(2l+m_iD_1+1)}(k)|^2}\right\} \\ &= \frac{1}{\bar{S}\bar{\gamma}} E_1\left(\frac{a_{\min}^2}{\bar{S}\sigma_C^2}\right) + \frac{1}{4\bar{S}^2\bar{\gamma}^2}\left\{E_1\left(\frac{a_{\min}^2}{\bar{S}\sigma_C^2}\right)\right\}^2,\ i=1,\,2 \end{aligned} \tag{18}$$

where $\bar{\gamma} = \sigma_C^2 E_s/\sigma_W^2$ is the average signal-to-noise ratio (SNR), $\bar{S} = E\{|S|^2\} \approx 1.04\,\text{dB}$, $E_1(a) = \int_a^\infty x^{-1}e^{-x}dx$ $(a > 0)$ is the exponential integral, and the probability of the amplitude $|C_{b(2l+m_iD_1)}(k)|$ exceeding a specific minimum level $a_{\min}$ is given by $e^{-a_{\min}^2/\sigma_C^2}$. Here, we assume that $|C_{b(2l+m_iD_1)}(k)|$ has the Rayleigh distribution as obtained in [10–12]. When $a_{\min}^2/\sigma_C^2 = -30\,\text{dB}$, for example, the 99.9% level of Rayleigh fading could be achieved.

Substituting (11) into (10) yields

$$E\left\{|\epsilon_\Delta|^2\right\} \approx \frac{1}{2\pi^2 N_u[K_{b(2l+m_1D_1)}+K_{b(2l+m_2D_1)}]^2(m_2-m_1)^2D_1^2\rho^2\bar{S}\bar{\gamma}} \cdot\left[E_1\left(\frac{a_{\min}^2}{\bar{S}\sigma_C^2}\right)+\frac{1}{4\bar{S}\bar{\gamma}}\left\{E_1\left(\frac{a_{\min}^2}{\bar{S}\sigma_C^2}\right)\right\}^2\right]. \quad (19)$$

It is noted that the performance enhancement of the proposed estimator is proportional to the increase of $m_2 - m_1$, while the estimation range is inversely proportional to the increase of $m_2 - m_1$.

4. SIMULATION RESULTS

In this section, extensive simulations are performed to verify the accuracy of the MSE analysis. In our simulations, 200 Mb/s UWB-OFDM system with $N = 128$, $N_u = 112$, and $\Delta_s = \pm 20$ ppm is chosen according to the UWB-OFDM specification, while Δ_r is assumed to be 20% for ± 20 ppm frequency tolerance [4]. The UWB channel models (CMs) are used for simulations [13] and a simple least square (LS) channel estimator is adopted. As a reference, we consider a pilot-aided conventional CFO estimation scheme developed in [7]

$$\hat{\Delta}_r = \frac{\sum_{i=1}^{N_p} \measuredangle\{R_{2l}^*(k_i)R_{2l+mD_2}(k_i)\}}{2\pi N_p K_{b(2l)} D_2 \rho} \quad (20)$$

where $N_p = 12$ is the number of pilots and D_2 is the minimum distance between non-zero identical parts of the pilot symbol transmitted in the same frequency band. Similarly, an average estimation over the different bands $\{b(2l)\}$ is applied, depending on the type of TFCs. To fairly evaluate the conventional and proposed approaches, $m_2 - m_1 = m = 1$ and $D_1 = D_2$ is adopted so that $(m_2 - m_1)D_1 = mD_2$ in the following examples.

Figure 2 plots the average estimate, $E[\hat{\Delta}_r]$, versus normalized CFO Δ_r as obtained with the two estimators under no additive noise in CM1. As shown in Figure 2, the estimates are practically unbiased within the allowed range around $\Delta_r = 0$, and reveals that error variance of the proposed algorithm is almost flat in the allowed region, i.e., $E[\hat{\Delta}_r] = \Delta_r$. As expected from (13) and (20), it is evident that the estimation range of the proposed CFO estimator is shortened by a factor of $\max[K_{b(2l+m_1D_1)} + K_{b(2l+m_2D_1)}]/\max[K_{b(2l)}]$, compared to that of the conventional scheme [7].

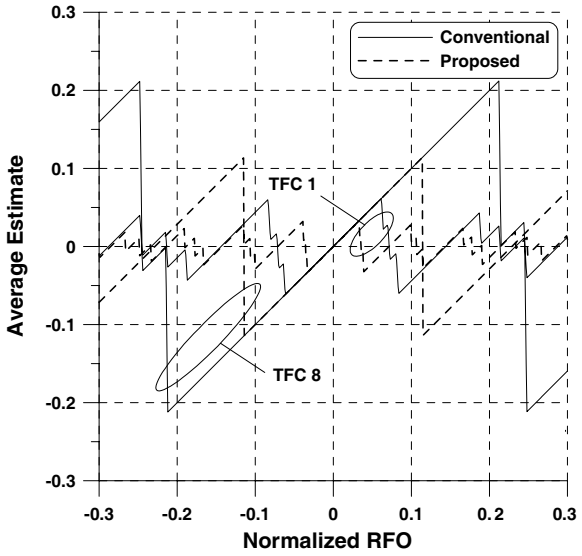

Figure 2. Average estimate of the CFO estimators in CM1.

Figure 3 presents the MSE performance of the proposed CFO estimator in CM1 when the receiver has perfect knowledge of the channel. In this example, $a_{\min}^2/\sigma_C^2 = -30\,\text{dB}$ is assumed. From this figure, we can observe that the MSE by simulation shows negligible difference with that of analytical derivation at the high SNR region.

The MSE performance of the CFO estimators in CM1 and CM2 is depicted in Figure 4 when LS estimation is used in (6). Although the signal is transmitted at one frequency band in the case of TFCs 5∼7, the conventional scheme is designed to have the average estimate over two temporal correlations with each having D_2 distance since the proposed scheme uses four OFDM symbols for synchronization. When compared to the conventional method in [7], the proposed method gives an improved estimation performance in terms of MSE. In comparison with the case of perfect CE as shown in Figure 3, it is observed that the performance of the proposed scheme gets worse at low SNRs when TFC1 is used. This is due to the fact that the estimation range in the case of TFC1 is much smaller than that in the case of other TFCs as confirmed by Figure 2, thus its performance becomes sensitive to the additive noise and channel estimation error. Performance improvement in CM3 and CM4, which is more dispersive than CM1 and CM2, is also observed in Figure 5.

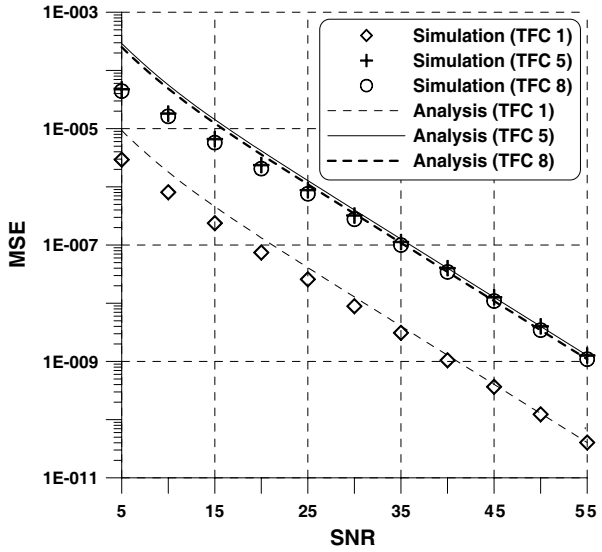

Figure 3. MSE performance of the proposed CFO estimator versus TFC in CM1.

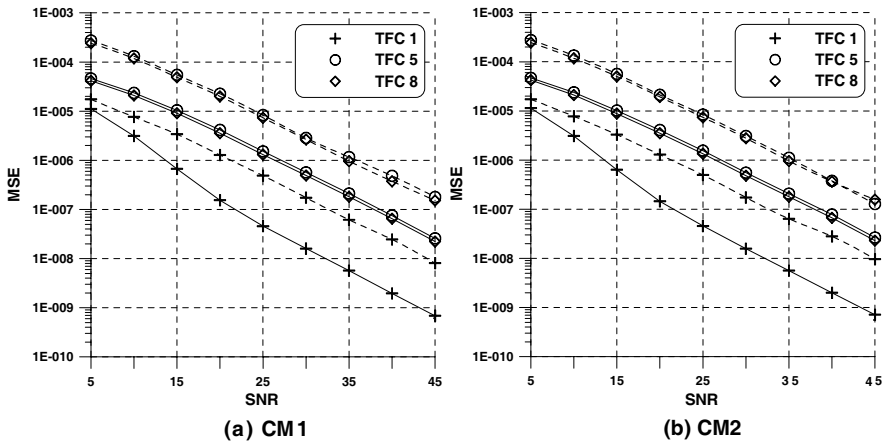

Figure 4. MSE performance of the CFO estimators versus TFC in CM1 and CM2: (1) solid lines — proposed, (2) dashed lines — conventional.

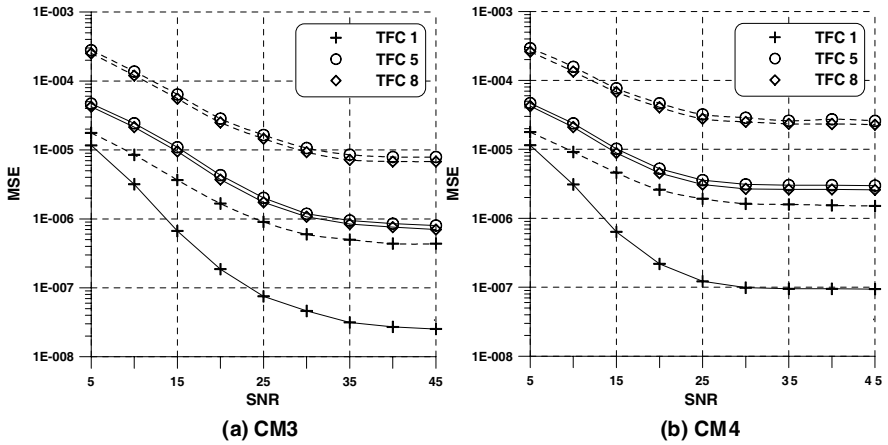

Figure 5. MSE performance of the CFO estimators versus TFC in CM3 and CM4: (1) solid lines — proposed, (2) dashed lines — conventional.

5. CONCLUSION

In this paper, we considered the issue of residual CFO estimation for an UWB-OFDM system. The estimation performance has been studied through the MSE analysis and a simple expression for the MSE has been obtained when the channel estimation is perfect. The error performance of the proposed estimator was compared with that of the conventional estimator. We also showed that the frequency estimator with the help of pilot and data symbols can be efficiently implemented in the UWB-OFDM system.

ACKNOWLEDGMENT

The authors wish to acknowledge the assistance and support of the Center for Advanced Transceiver Systems and the Ministry of Knowledge Economy, and this research is supported by Seoul R&BD Program.

REFERENCES

1. Aiello, G. R. and G. D. Rogerson, "Ultra-wideband wireless systems," *IEEE Microwave Mag.*, Vol. 4, 36–47, Jun. 2003.

2. Win, M. Z. and R. A. Scholtz, "On the robustness of ultra-wide bandwidth signals in dense multipath environments," *IEEE Commun. Lett.*, Vol. 2, 51–53, Feb. 1998.
3. Cramer, R. J. M., R. A. Scholtz, and M. Z. Win, "Evaluation of an ultrawideband propagation channel," *IEEE Trans. Antennas Propagat.*, Vol. 50, 561–570, May 2002.
4. Xiao, S.-Q., J. Chen, B.-Z. Wang, and X.-F. Liu, "A numerical study on time-reversal electromagnetic wave for indoor ultra-wideband signal transmission," *Progress In Electromagnetics Research*, PIER 77, 329–342, 2007.
5. Lie, J. P., B. P. Ng, and C. M. See, "Multiple UWB emitters DOA estimation employing time hopping spread spectrum," *Progress In Electromagnetics Research*, PIER 78, 83–101, 2008.
6. Liu, X.-F., B.-Z. Wang, S.-Q. Xiao, and J. H. Deng, "Performance of impulse radio UWB communications based on time reversal technique," *Progress In Electromagnetics Research*, PIER 79, 401–413, 2008.
7. ECMA International, Standard ECMA-368, "High rate ultra wideband PHY and MAC standard," Dec. 2007.
8. Shim, E. S. and Y. H. You, "Parameter estimation and error reduction in multicarrier systems by time-domain spreading," *Progress In Electromagnetics Research B*, Vol. 7, 1–12, 2008.
9. Nam, S. H., J. S. Yoon, and H. K. Song, "An elaborate frequency offet estimation for OFDM systems," *Progress In Electromagnetics Research Letters*, Vol. 4, 33–41, 2008.
10. Png, K.-B., X. Peng, S. Chattong, H. T. Francis, and F. Chin, "Joint carrier and sampling frequency offset estimation for MB-OFDM UWB system," *Proc. of RWS 2008*, 29–32, Jan. 2008.
11. Li, Y., T. Jacobs, and H. Minn, "Frequency offset estimation for MB-OFDM-based UWB systems," *Proc. of ICC 2006*, 4729–4734, Jun. 2006.
12. Liu, S. and J. Chong, "A study of joint tracking algorithms of carrier frequency offset and sampling clock offset for OFDM-based WLANs," *Proc. Int. Conf. Communications, Circuits, Systems, West Sino Expositions*, 109–113, Jul. 2002.
13. Gault, S., W. Hachem, and P. Ciblat, "Joint sampling clock offset and channel estimation for OFDM signals: Cramer-Rao bound and algorithms," *IEEE Trans. Signal Processing*, Vol. 54, No. 5, 1875–1885, May 2006.
14. Speth, M., S. A. Fechtel, G. Fock, and H. Meyr, "Optimum receiver design for wireless broad-band systems using OFDM —

Part I," *IEEE Trans. Commun.*, Vol. 47, No. 11, 1668–1677, Nov. 1999.

15. Wessman, M., A. Svensson, and E. Agrell, "Frequency diversity performance of coded multiband-OFDM systems on IEEE UWB channels," *Proc. of VTC 2004*, 1197–1201, Sept. 2004.
16. Koo, B.-W., M.-S. Baek, and H.-K. Song, "Multiple antenna transmission technique for UWB system," *Progress In Electromagnetics Research Letters*, Vol. 2, 177–185, 2008.
17. Kay, S. M., "A fast and accurate single frequency estimator," *IEEE Trans. Acoust., Speech, Signal Processing*, Vol. 37, 1987–1990, Dec. 1989.
18. Snow, C., L. Lampe, and R. Schober, "Performance analysis and enhancement of multiband OFDM for UWB communications," *IEEE Trans. Wireless Commun.*, Vol. 6, No. 6, 2182–2192, Jun. 2007.
19. Foerster, J., et al., Channel modeling sub-committee report, IEEE P802.15-02/490r1-SG3a, Mar. 2003.